Neurosci. Bull. January, 2024, 40(1):17–34
https://doi.org/10.1007/s12264-023-01094-x

www.neurosci.cn
www.springer.com/12264

ORIGINAL ARTICLE

TREM-2 Drives Development of Multiple Sclerosis by Promoting Pathogenic Th17 Polarization

Siying Qu[1] · Shengfeng Hu[2] · Huiting Xu[1] · Yongjian Wu[1] · Siqi Ming[1] · Xiaoxia Zhan[3] · Cheng Wang[4] · Xi Huang[1]

Received: 7 January 2023 / Accepted: 7 May 2023 / Published online: 27 July 2023

Abstract Multiple sclerosis (MS) is a neuroinflammatory demyelinating disease, mediated by pathogenic T helper 17 (Th17) cells. However, the therapeutic effect is accompanied by the fluctuation of the proportion and function of Th17 cells, which prompted us to find the key regulator of Th17 differentiation in MS. Here, we demonstrated that the triggering receptor expressed on myeloid cells 2 (TREM-2), a modulator of pattern recognition receptors on innate immune cells, was highly expressed on pathogenic CD4-positive T lymphocyte ($CD4^+$ T) cells in both patients with MS and experimental autoimmune encephalomyelitis (EAE) mouse models. Conditional knockout of *Trem-2* in $CD4^+$ T cells significantly alleviated the disease activity and reduced Th17 cell infiltration, activation, differentiation, and inflammatory cytokine production and secretion in EAE mice. Furthermore, with *Trem-2* knockout *in vivo* experiments and *in vitro* inhibitor assays, the TREM-2/zeta-chain associated protein kinase 70 (ZAP70)/signal transducer and activator of transcription 3 (STAT3) signal axis was essential for Th17 activation and differentiation in EAE progression. In conclusion, TREM-2 is a key regulator of pathogenic Th17 in EAE mice, and this sheds new light on the potential of this therapeutic target for MS.

Keywords Multiple sclerosis · Experimental autoimmune encephalomyelitis · T helper 17 · Triggering receptor expressed on myeloid cells 2

Introduction

Multiple sclerosis (MS) is a chronic inflammatory, demyelinating, and neurodegenerative disease of the central nervous system (CNS) [1]. According to the Atlas of MS database, ~2.5 million people suffer from MS worldwide. However, currently, no curative treatment is available [2]. The pathogenesis of MS has been attributed to a breakdown of T lymphocyte tolerance to CNS self-antigens, resulting in chronic inflammation with subsequent demyelination and neurodegeneration [3]. The imbalance and balance of T helper (Th) subsets lead to the onset and remission condition of the disease [4]. Among them, T helper 17 (Th17) cells play a prominent role in the progression of MS. During MS development, Th17 cells infiltrate into the CNS and produce interleukin-17 (IL-17), IL-6, and granulocyte-macrophage colony-stimulating factor (GM-CSF) to induce inflammation [5]. Another T cell subset, regulatory T cells (T_{reg}) take part

Siying Qu, Shengfeng Hu, and Huiting Xu contributed equally to this work.

Supplementary Information The online version contains supplementary material available at https://doi.org/10.1007/s12264-023-01094-x.

✉ Xi Huang
huangxi6@mail.sysu.edu.cn

1 Center for Infection and Immunity and Guangdong Provincial Engineering Research Center of Molecular Imaging, The Fifth Affiliated Hospital of Sun Yat-sen University, Zhuhai 519000, China

2 The State Key Laboratory of Respiratory Disease, Guangdong Provincial Key Laboratory of Allergy and Clinical Immunology, The Second Affiliated Hospital, Guangzhou Medical University, Guangzhou 510260, China

3 Department of Laboratory Medicine, The First Affiliated Hospital of Sun Yat-sen University, Guangzhou 510080, China

4 Division of Nephrology, Department of Medicine, the Fifth Affiliated Hospital of Sun Yat-sen University, Zhuhai 519000, China

in the remission stage of MS by restraining an excessive effector T cell response [6].

The activation and maturation of Th17 cells are complicated, with adequate T cell receptor (TCR) expression, co-stimulatory molecules, and cytokines. Prior to TCR recognition of the antigenic peptides presented by antigen-presenting cells, zeta-chain-associated protein kinase 70 (ZAP70) predominantly resides within the cytoplasm, where it is autoinhibited [7]. After TCR triggering, immunoreceptor tyrosine-based activation motif (ITAM)/ζ chain of the T-cell receptor (CD3ζ) and lymphocyte-specific protein tyrosine kinase (LCK) phosphorylation levels maintain sufficient intensity and duration [7, 8]. The autoinhibited conformation of ZAP70 is disrupted by binding to phosphorylated ITAMs [9]. The active conformation of ZAP70 is further stabilized through the phosphorylation of its interdomain linker and activation loop by LCK [10, 11]. Many cytokines that regulate Th17 development, including IL-6, IL-21, and IL-23, may signal through the signal transducer and activator of transcription 3 (STAT3) [12–14]. IL-6 synergizes with interleukin-6 receptor (IL-6R) to regulate Th17 cell differentiation and to maintain cytokine expression in effector Th17 cells [15]. Many findings suggest that IL-6-dependent STAT3 signaling is critical for autoimmune responses. Hyperactivation of STAT3 in patients with MS has been reported and this is correlated with disease progression [16]. In inflammatory bowel disease, IL-6/STAT3 signaling is an important regulator of the proliferation of pathogenic cells [17, 18]. Furthermore, the number of Th17 cells, as well as Th17-related cytokines such as IL-17 and IL-6, are increased in patients with systemic lupus erythematosus [19]. The T_{reg} cells have been reported to promote remission of MS by restraining the Th17 response. However, the clinical trials based on T_{reg} did not succeed as expected [20] because the imbalance of Th subsets was regulated by other immune cells and the immune environment. Therefore, the upstream regulation of Th17 differentiation might be the key to the development of a therapeutic target for MS.

Multiple pattern recognition receptors, such as the toll-like receptor (TLR) and triggering receptor expressed on myeloid cell (TREM), were necessary for antigen presentation and the differentiation of T cells [21]. In previous studies, TREM family members were widely expressed in myeloid cells, such as macrophages, monocytes, and dendritic cells [22]. Among this family, TREM-1 and TREM-2 are typical members that can interact with the ITAM-containing adapter DNAX activation protein of 12 kDa (DAP12) to exert their respective functions. TREM-1 plays a pro-inflammatory role by amplifying TLR signaling. TREM-2 exhibits a multifunctional phenotype in infectious and inflammatory diseases, which may depend on complex ligands and signal pathways. Lipids (exposed upon axonal injury), nucleic acids (released by dying cells), and proteins (expressed on cell and bacterial surfaces and heat shock proteins) have been proposed to potentially bind to TREM-2 [23, 24]. It has been reported that TREM-2 has anti-inflammatory effects on the innate immune cells during infectious and inflammatory diseases. On one hand, TREM-2 regulates the inflammatory response in a mouse model of sepsis induced by Gram-negative bacteria [24]. For example, in the liver injury model induced by chemical agents, liver injury and inflammation are aggravated in TREM-2 deficient (*Trem-2*$^{-/-}$) mice [25]. On the other hand, TREM-2 promotes inflammation and amplifies immune responses in some diseases. For example, the inflammatory response, organ damage, and death rate caused by *Burkholderia pseudomallei* infection were decreased in TREM-2 deficient mice [26]. From our previous research, TREM-2 promotes the pro-inflammatory Th1 response through CD3ζ/ZAP70 in *Mycobacterium tuberculosis* [27] and SARS-CoV-2 [28] infection, which indicated that TREM-2 also plays a crucially important role in Th cells.

In addition to its critical role in infectious diseases, TREM-2 also plays an important role in neural diseases. As per previous reports, TREM-2 and DAP12 are predominantly expressed by microglia. Moreover, microglial dysfunction caused by TREM-2/DAP12 impairment is involved in the pathogenesis of Nasu-Hakola disease. The variant of TREM-2 (loss-of-function mutation, R47H) may lead to a predisposition to Alzheimer's disease and frontotemporal dementia [29, 30]. TREM-2 activation attenuates neuroinflammation and neuronal apoptosis after intracerebral hemorrhage, mediated by activation of the phosphatidylinositol 3-kinase (PI3K)/v-akt murine thymoma viral oncogene homolog (Akt) signaling pathway [31]. The imbalance of TREM-2 inhibits the lipopolysaccharide-induced neuroinflammatory response in BV-2 cells [32]. However, unlike *Dap12* knockout (*Dap12*$^{-/-}$) mice (fewer microglia and aberrant morphology), *Trem-2*$^{-/-}$ mice show no spontaneous abnormalities in myelin, even in aged mice. The protective effect of TREM-2 for myelin maintenance relies on DAP12. In MS, the soluble myeloid trigger receptor-2 level is increased in cerebrospinal fluid (CSF) and is considered a new marker of microglial activation [33]. Appropriate microglial activation contributes to myelin clearance, which is thought to be required for remyelination [34]. In a model of MS, experimental autoimmune encephalomyelitis (EAE), excessive activation of microglia is detrimental to regeneration [35]. However, a controversial result has been obtained. DAP12-deficient mice have been shown to be highly resistant to EAE. This may be because TREM-2 is one of the DAP12-associated receptors. With more ligands of TREM-2, such as ZAP70, TREM-2 may not always play a neuroprotective role in MS. In conclusion, previous studies of TREM-2 all focused on the myeloid cells, especially

microglia in the CNS. Nevertheless, its function in the Th cells of the peripheral immune system is not clear.

In the present study, we reported that TREM-2 was highly expressed in the $CD4^+$ T cells from patients with MS and from EAE mice. With *Trem-2* conditional knockout and adoptive T cell experiments, we found that TREM-2 regulated Th17 activation, differentiation, and Th17-related cytokine secretion. In $CD4^+$ T cells, ZAP70 phosphorylation was triggered by TREM-2 and promoted the activation of STAT3. TREM-2 promoted Th17 polarization through the ZAP70/STAT3 signal pathway during EAE. This study sheds new light on the promise of regulating the pro-inflammatory Th17 response to treat MS.

Materials and Methods

Patients with MS and Healthy Controls

We enrolled 12 relapsing-remitting patients with MS (based on the 2010 McDonald diagnostic criteria) from the Nanfang Hospital of Southern Medical University. We also recruited 12 controls without inflammatory diseases. The demographic and clinical features of the participants are listed in Table 1. Patients enrolled in the database were diagnosed by 2 specialized neurologists. All procedures were approved by the Fifth Affiliated Hospital of Sun Yat-sen University and were performed according to the National Institutes of Health Guide for the Care and Use of Laboratory Animals (ZDWY.XBZLK.011).

Preparation of Peripheral Blood Samples

After the collection of 2 mL of EDTA-anticoagulated blood, we immediately centrifuged all samples to obtain serum samples. Peripheral blood mononuclear cells were isolated using lymphocyte separation medium (Beyotime Biotechnology, Shanghai, China).

Table 1 Demographic and clinical features of patients with MS and healthy controls

	MS ($n = 12$)	CTLs ($n = 12$)
Gender (female/male)	8/4	7/5
Age[1] (years)	33.25 (19–55)	35.64 (22–57)
Age at onset (years)	30 (16–48)	n.a.
Disease duration[2] (years)	0.48 (0.1–1)	n.a.
EDSS score	3.75 (2–7.5)	n.a.

Values indicate the mean (range) unless otherwise indicated

CTLs controls, *EDSS* Expanded Disability Status Scale, *MS* multiple sclerosis, *n.a.* not available

[1]At the sampling time point

[2]From disease onset to sampling

Mice

Female C57BL/6 mice (4–6 weeks old) were purchased from Guangdong Medical Laboratory Animal Center. *Rag2* knockout ($Rag2^{-/-}$) mice were purchased from Guangzhou Sebiona Biological Science and Technology Co. Ltd (Guangzhou, China). *Trem-2* knockout ($Trem\text{-}2^{-/-}$) mice were generously provided by Marco Colonna (Washington University, USA). *Cd4* conditional knockout *Trem-2* ($Cd4^{Cre}Trem\text{-}2^{flox}$) mice were generated by $Trem\text{-}2^{flox/flox}$ and *Cd4-Cre* mice. $Trem\text{-}2^{flox/flox}$ mice were from the Model Animal Research Center (Nanjing, China); *Cd4-Cre* mice were purchased from the Jackson Laboratory (Sacramento, USA), stock no. 022071. Mice were housed at room temperature (23 ± 1 °C) with a 12-h/12-h light-dark cycle and with *ad libitum* access to food and water. All experimental procedures were approved by the Fifth Affiliated Hospital of Sun Yat-sen University Ethics Committee (2021.00156).

Data Re-analysis

Re-analysis data were from the Gene Expression Omnibus (GEO; https://www.ncbi.nlm.nih.gov/geo/). The GEO accession numbers of Human Bulk-RNA sequencing data were GSE66763, and for *Mus musculus*, GSE57098. We used the average value of messenger RNA (mRNA) expression as the expression value for that sample. For heatmap representation, the normalized expression of each mRNA was used.

Cell Preparation and Culture

Lymphocytes from the spleen and lymph nodes were collected under sterile conditions. Cell suspensions were ground and filtered with 40 μm nylon mesh strainers. Then the cells were held in ice-cold Roswell Park Memorial Institute (RPMI) 1640 medium for subsequent experiments.

Cells were incubated in RPMI 1640 (2×10^6 cells/mL) with $MOG_{35–55}$ (20 μg/mL) in a humidified incubator at 37 °C with 5% CO_2 for 48 h. The RPMI 1640 medium was supplemented with 10% fetal bovine serum, 2 mmol/L L-glutamine, 1 mmol/L sodium pyruvate, 100 IU/mL penicillin/streptomycin, and 2×10^{-5} mol/L 2-methylimidazole (2-ME) (Life Technologies, Carlsbad, CA, USA).

Flow Cytometry Analysis

For surface staining, cells were washed and stained for 30 min with fluorescently conjugated monoclonal antibodies (mAbs). The mAbs of human targets for flow cytometry were as follows: FITC-CD4 [catalog number (CAT):

317408, Biolegend, San Diego, USA], Percp-cy5.5-CD3 (CAT: 344813, Biolegend), APC-CD8 (CAT: 980904, Biolegend), PE-TREM-2 (CAT: FAB17291P, BD, New Jersey, USA). The mAbs of mice were as follows: FITC-CD3 (CAT: 110204, Biolegend), PE-cy7-CD4 (CAT: 100421, Biolegend), Pacific blue-CD8 (CAT: 100725, Biolegend), PE-TREM-2 (CAT: FAB17291P, BD), APC-cy7-CD62L (CAT: 104427, Biolegend), APC-CD69 (CAT: 104513, Biolegend), CD11c-PEcy7 (CAT: 117318, Biolegend), F4/80-APC (CAT: 123116, Biolegend). For intracellular staining, cells were stimulated for 6–8 h at 37 °C in 5% CO_2. To detect cytokines, Brefeldin A (BFA) (Sigma, St. Louis, USA, 10 μg/mL) was added after 4 h. After stimulation, cells were washed in cold phosphate-buffered saline (PBS). Cell surface staining was applied followed by fixation/permeabilization (CAT: 00-5123-43, eBioscience, San Diego, USA) and stained with the antibodies: IFN-γ-V450 (CAT: 560371, BD Biosciences), TNF-APC (CAT: 506307, Biolegend), IL-6-APC (CAT: 504507, Biolegend), IL-17-APC-cy7 (CAT: 506939, Biolegend), IL-4-PEcy7 (CAT: 504118, Biolegend), STAT3-PE (CAT: 612569, BD Biosciences), pZAP70-Pc5.5 (CAT: 693809, Biolegend) or their corresponding isotype controls. Cell phenotype was tested using a FACS Calibur instrument (BD LSR II, USA). The BD Influx^{TM} machine (BD Biosciences) and Sony MA900, Tokyo, Japan) were used for cell sorting, including $CD4^+$ T and $CD8^+$ T cells. The data were analyzed by FlowJo-V10 (BD).

Thymidine Incorporation Assay

The proliferation of mouse $CD4^+$ T cells was measured by the incorporation of [3H]thymidine. Briefly, purified $CD4^+$ T cells were incubated for 48 h with increasing concentrations of plate-bound anti-CD3 in wells. During the final 8 h of stimulation, [3H]thymidine was added to the medium. The amount of incorporated [3H]thymidine was measured as counts per minute. The instrument we used was from Beckman (8100 LS beta-counter) (Beckman, Bria, USA).

$CD4^+$ T Cell Transfer

Spleens were isolated from wild-type (WT) and *Trem-2*$^{-/-}$ mice. Then $CD4^+$ T cells were purified with CD4 microbeads and autoMACS (CAT: 130-104-454, Miltenyi, Bergisch Gladbach, Germany). $CD4^+$ T cells were counted and washed 3 times with PBS. Single-cell suspensions were then injected into the tail veins of *Rag2*$^{-/-}$ mice at 5×10^6 cells per mouse. EAE was induced after mice were immunized the day following $CD4^+$ T cell transfer.

Real-Time Quantitative Polymerase Chain Reaction (RT-qPCR)

Total RNA was isolated with TRIzol reagent (Thermo Fisher Scientific, Massachusetts, USA). First-strand complementary DNA (cDNA) was obtained with a Synthesis Kit (Thermo Fisher Scientific); 2 μL of total cDNA and Synergy Brands (SYBR) Green PCR Master Mix (Applied Biosystems, Massachusetts, USA) were mixed. Then Eppendorf Master Cycle Realplex2 was used for real-time PCR (40 cycles). The RT-qPCR conditions were as follows: 3 min of enzyme activation at 95 °C, followed by denaturation at 95 °C for 20 s and annealing of primers at 60 °C for 20 s, and extension at 72 °C for 20 s. qPCR data were analyzed by the ΔΔCT method.

Enzyme-Linked Immunosorbent Assay (ELISA)

Cytokines secreted by $CD4^+$ T cells were quantified by a two-site enzyme-linked immunosorbent assay (Dakewee Bio-engineering Co., Ltd, Shenzhen, China). The kits used were as follows: Human IL-17 Quantikine ELISA kit (CAT: 1111702, Dakewe), Human TNF Quantikine ELISA kit (CAT: 1117202, Dakewe), Human GM-CSF Quantikine ELISA kit (CAT: 1117302, Dakewe), Human IFN-γ Quantikine ELISA kit (CAT: 1110002, Dakewe), Mouse IL-17 Quantikine ELISA kit (CAT: 1111703, Dakewe), Mouse IFN-γ Quantikine ELISA kit (CAT: 1210002, Dakewe), Mouse IL-6 Quantikine ELISA kit (CAT: 1210602, Dakewe) and Mouse TNF-α Quantikine ELISA kit (CAT: 1211702, Dakewe).

Western Blotting

Cells were washed with PBS and prepared using radio immunoprecipitation assay (RIPA) buffer. After electrophoresis, proteins were electroeluted onto a polyvinylidene fluoride (PVDF) membrane. After blocking with 5% non-fat dry milk in phosphate buffered solution with Tween (PBST), the membranes were incubated overnight with primary antibodies at 4 °C [CAT: 91068 (TREM-2); 9139 (STAT3); 9145 (pSTAT3); 3165 (ZAP70); 2701 (pZAP70); 93473 (β-Actin), Cell Signaling Technology, Boston, USA]. Then appropriate horseradish peroxidase (HRP)-conjugated secondary antibodies were chosen to incubate with the membranes. The membranes were visualized with Plus-ECL (CAT: NEL102001EA, PerkinElmer, CA, USA).

EAE Model

Mice were immunized with $MOG_{35–55}$ (MEVGWYRSPFSRVVHLYRNGK) (CAT: BYX-P-003, Bioyears, Wuhan, China) and complete Freund's adjuvant (CFA) (Difco

Laboratories, Massachusetts, USA). Briefly, $MOG_{35–55}$/CFA emulsion was injected subcutaneously in the armpits of their forelimbs (0.1 mL/mice). Pertussis toxin (List Biological Laboratories, Inc., Campbell, CA) was injected i.p. on the day of immunization and 48 h later. Weight and clinical scores were monitored every two days. The following standard EAE scoring system was applied: (0) no disease, (1) floppy tail, (2) hind limb weakness, (3) full hind limb paralysis, (4) quadriplegia, and (5) death. Mice with intermediate-level presentations were scored in increments of 0.5. Mice with a clinical core between 3.5 and 4.5 were considered to have reached the peak of the disease.

Statistical Analysis

Statistical analysis of the data was carried out with GraphPad Prism 8.0.2 software (GraphPad Software, San Diego, USA), using Student's *t*-test. Differences between groups were considered significant at $P < 0.05$.

Results

The Expression of TREM-2 and Th17-Related Cytokines Are Up-Regulated in the Peripheral CD4$^+$ T Cells of Patients with MS

To explore the heterogeneity between MS CD4$^+$ T cells and healthy CD4$^+$ T cells, mRNA sequencing data (GEO, database ID GSE66763) of these two types of CD4$^+$ T cells were analyzed. Th17-related cytokines (IL-17, TNF, GM-CSF, and IFN-γ) were significantly increased in CD4$^+$ T cells from patients with MS (Fig. 1A, MS: $n = 4$; Healthy: $n = 5$, *IL17A*: $P < 0.001$; *IL17F*: $P = 0.012$; *TNF*: $P = 0.162$; *GM-CSF*: $P < 0.001$; *IFNG*: $P < 0.001$). The concentrations of these cytokines were significantly increased in the peripheral blood of patients with MS (Fig. 1B, $n = 7$, IL-17: $P = 0.009$; TNF: $P = 0.082$; GM-CSF: $P = 0.031$; IFN-γ: $P = 0.041$). These results indicated that Th17 plays an important role in MS; this is consistent with previous studies [36]. To further explore the regulatory mechanism of Th17 *versus* naïve T cells, TREM family expression was analyzed (Fig. 1C, $n = 3$, *TREM-1*: $P = 0.221$; *TREML-1*: $P = 0.109$; *TREM-2*: $P = 0.011$; *TREML-2*: $P = 0.501$; *TREM-3*: $P = 0.135$; *TREML-4*: $P = 0.869$). Compared with naïve T cells, *TREM-2* was highly expressed in Th17 cells. However, other TREMs,

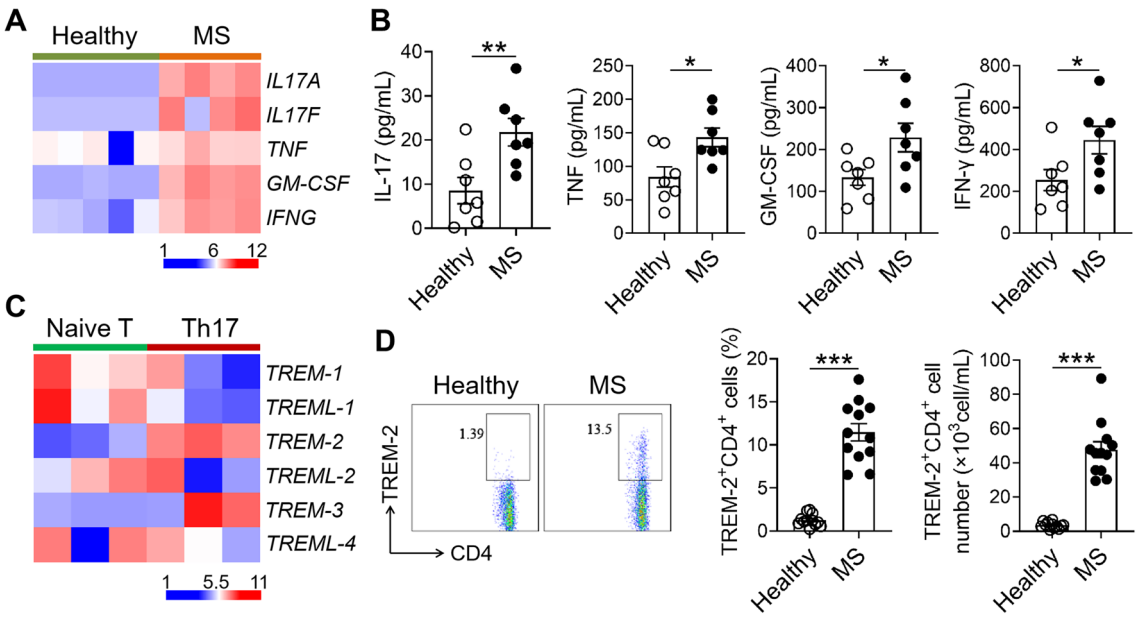

Fig. 1 CD4$^+$ T cells from MS peripheral blood express higher Th17-related factors and TREM-2. **A** Heatmap showing *IL17A, IL17F, TNF, GM-CSF*, and *IFNG* mRNA expression (MS: $n = 4$; Healthy: $n = 5$). Red means relatively up-regulated genes, and blue means relatively down-regulated genes. **B** Production of cytokines (IFN-γ, IL 17, TNF-α, and GM-CSF) in serum from patients with MS and healthy controls as detected by ELISA ($n = 7$). **C** Heatmap of the mRNA expression of *TREM* family members (*TREM-1, TREML-1, TREM-2, TREML-2, TREM-3*, and *TREML-4*) ($n = 3$). Red means relatively up-regulated genes, and blue means relatively down-regulated genes. **D** Frequency of TREM-2 on CD4$^+$ T cells and number of TREM-2$^+$CD4$^+$ T cells in the human peripheral blood CD4$^+$ T cells from MS ($n = 12$). For **B** and **D**, Student's *t*-test was used and the data are shown as the mean ± SEM. *$P < 0.05$, **$P < 0.01$, ***$P < 0.001$

including *TREM-1*, *TREML-1*, *TREML-2*, *TREM-3*, and *TREML-4* did not significantly differ in Th17 *versus* naïve T cells. Meanwhile, the proportion and number of peripheral TREM-2$^+$CD4$^+$ T cells were significantly increased in patients with MS (Fig. 1D, $n = 12$, frequency: $P < 0.001$; absolute number: $P < 0.001$). These results suggested that the progression of MS may be associated with TREM-2 and Th17 cells.

Increasing TREM-2$^+$CD4$^+$ T Cells Are Positively Correlated with the Progression of the EAE Model

EAE is the most commonly used experimental model for MS. We then established EAE- and completed Freund's adjuvant-induced (CFA, control group) mouse models of MS and inflammatory pain, respectively. Then we analyzed the proportions of TREM-2-positive cells among CD4$^+$ T cells (CD3$^+$CD4$^+$), cytotoxic T lymphocytes (CTLs; CD3$^+$CD8$^+$), B cells (CD3$^-$CD19$^+$), and macrophages (CD3$^-$CD11c$^+$F4/80$^+$) in their spleen and lymph nodes (axillary, inguinal, para-aortic, and mesenteric nodes) (Fig. 2A–D, $n = 6$, Th cells in spleen: $P = 0.025$; Th cells in para-aortic nodes: $P = 0.014$). Compared with the CFA group, TREM-2$^+$CD4$^+$ T cells were significantly increased in the spleen of EAE mice. However, there was no significant difference in TREM-2$^+$cells among other immune cells between CFA and EAE mice. These results matched those of human samples (Fig. 1D). In order to match the characteristics of MS [37], we divided the process of EAE into three stages: the early stage, the onset stage, the peak stage, and the recovery stage based on the clinical scores (Fig. 2E, $n = 12$, $P < 0.001$). At the peak stage of the disease, the proportion of TREM-2$^+$CD4$^+$ T cells in the spleen also reached its peak value (Fig. 2F, $n = 6$, $P < 0.001$). Furthermore, there was a positive correlation between clinical score and the proportion of TREM-2$^+$CD4 cells measured (Fig. 2G, $n = 38$, $R^2 = 0.873$, $P < 0.001$). As MS/EAE are demyelinating diseases that affect the CNS, we also examined the expression of TREM-2 on CD 4$^+$T cells in the CNS (brain and spinal cord) (Fig. 2H, $n = 6$, brain: $P < 0.001$; spinal cord: $P < 0.001$). The results showed that the expression of TREM-2 on T cells in the CNS of EAE mice was higher than that of CFA mice. These results suggested that the expression of TREM-2 on CD4$^+$ T cells is correlated with disease progression.

TREM-2 Is Essential for CD4$^+$ T Cell Pathogenicity and EAE Induction

In order to confirm that the TREM-2$^+$CD4$^+$ T cell is essential for EAE induction, we used *Cd4* conditional knockout *Trem-2* (*Cd4*^{Cre}*Trem-2*^{flox}) mice to establish the EAE model. The clinical scores of wild-type (WT)-CFA, WT-EAE, and *Cd4*^{Cre}*Trem-2*^{flox}-EAE mice were monitored after EAE induction with $MOG_{35–55}$. The clinical score of *Cd4*^{Cre}*Trem-2*^{flox}-EAE mice was lower than that of WT-EAE mice (Fig. 3A, $n = 12$, $P < 0.001$). We then injected Evans blue (EB) *via* the tail vein to check their blood-brain barrier (BBB) integrity. The results showed that the spinal cord of WT-EAE mice was significantly greater than that of *Cd4*^{Cre}*Trem-2*^{flox}-EAE mice. The highest EB level in the spinal cord of WT-EAE mice was indicative of more BBB damage than that of *Cd4*^{Cre}*Trem-2*^{flox}-EAE mice that had a low EB level (Fig. 3B, $n = 6$, CFA *vs* EAE: $P = 0.031$, EAE *vs* *Cd4*^{Cre}*Trem-2*^{flox}-EAE: $P = 0.020$). Hematoxylin/eosin staining showed that *Trem-2* knockout reduced inflammatory cell infiltration and tissue injury in the brain (Fig 3C). In addition, flow cytometry showed that Th cell infiltration was reduced in the brain and spinal cord of *Cd4*^{Cre}*Trem-2*^{flox}-EAE mice compared with those of WT-EAE (Fig 3D, $n = 6$, brain WT-EAE *vs* *Cd4*^{Cre}*Trem-2*^{flox}-EAE: $P = 0.016$; spinal cord WT-EAE *vs* *Cd4*^{Cre}*Trem-2*^{flox}-EAE: $P = 0.008$). These findings indicated that TREM-2 deficiency in CD4$^+$ T cells impairs the pathogenesis of EAE. To evaluate the direct role of TREM-2 in the regulation of CD4$^+$ T cell pathogenicity *in vivo*, *Rag2* knockout (*Rag2*$^{-/-}$) mice were reconstituted with CD4$^+$ T cells from WT-EAE or *Trem-2* knockout (*Trem-2*$^{-/-}$)-EAE mice (Fig. 3E). Mice reconstituted with WT CD4$^+$ T cells exhibited substantially higher disease severity than mice reconstituted with *Trem-2*$^{-/-}$ T cells (Fig. 3F, $n = 6$, $P < 0.001$). These results indicated that TREM-2 promotes the pathogenicity of CD4$^+$ T cells in the EAE model.

TREM-2 Regulates the Expression of Th17 Cell-related Genes After Immunization

In human samples, we found that TREM-2 was positively correlated with the Th17-related gene expression level (Fig. 1). Thus, we investigated the role of TREM-2 in regulating Th17 cells. Firstly, we checked the number and proportion of double-negative T cells, double-positive T cells, CD4$^+$ T cells, and CD8$^+$ T cells in the thymus of *Trem-2*$^{-/-}$ mice (Fig. S1A–C). The results showed that TREM-2 deficiency did not affect T cell development. Immune organ (thymus and spleen) weight did not change in *Trem-2*$^{-/-}$ mice (Fig. S1D). In the lymph nodes and spleen, mature immune cells, including CD 4$^+$T cells, CD8$^+$T cells, CD19$^+$B cells, and macrophages, were also not affected in *Trem-2*$^{-/-}$ mice (Fig. S1E, F). T-cell thymidine incorporation was conducted *in vitro*. There was no difference in proliferation between WT and *Trem-2*$^{-/-}$ CD4$^+$ T cells (Fig. S1G, H). The results indicated that TREM-2 does not affect CD4$^+$ T development in the physiological state.

Next, we reanalyzed mRNA sequencing data between Naïve T *vs* three subsets of Th17 cells [38]. These four

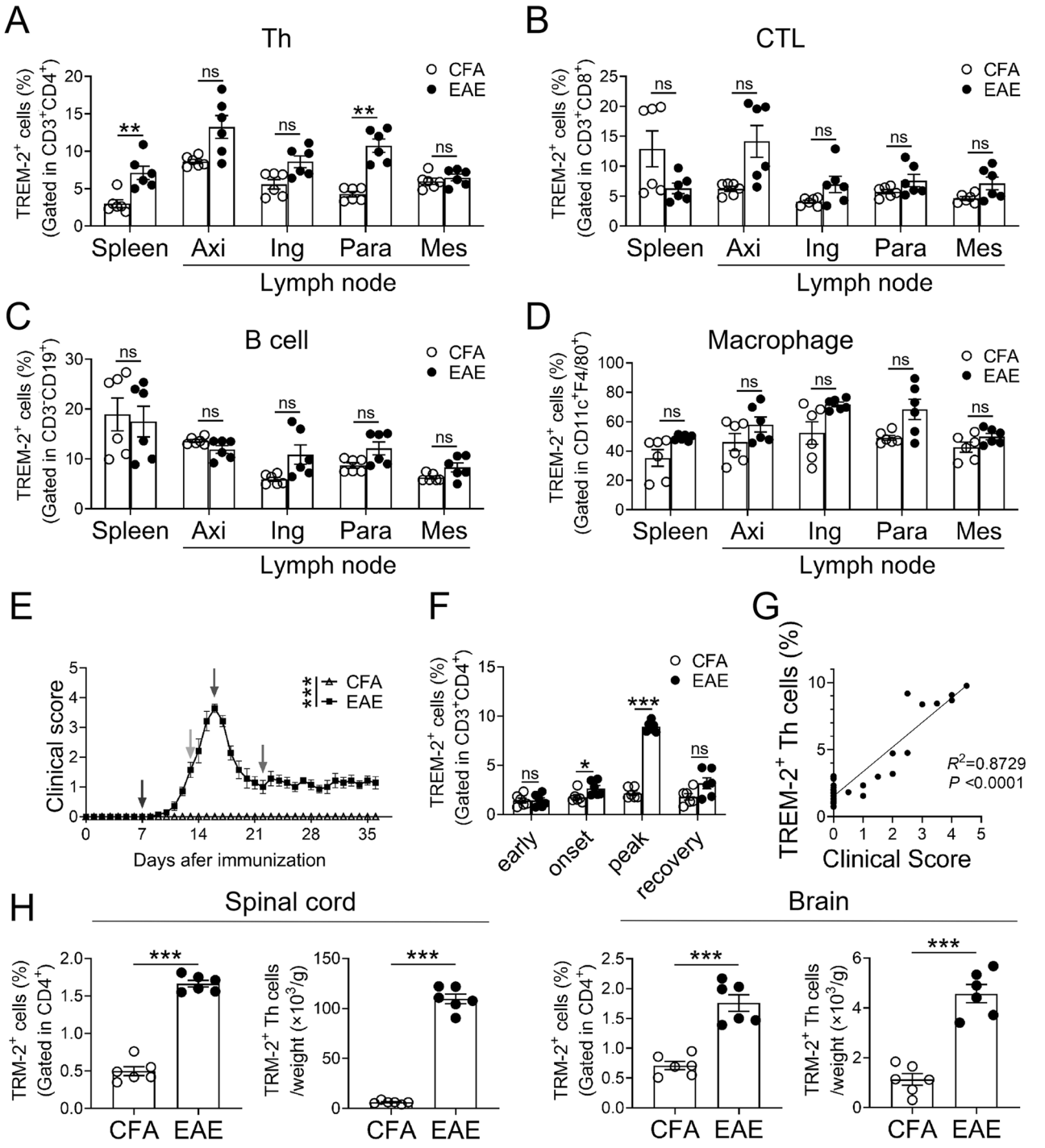

Fig. 2 High TREM-2 expression on $CD4^+$ T cells is significantly correlated with EAE progression. **A–D**, The percentages of TREM-2-positive cells after EAE induction in $CD4^+$ T cells (**A**), $CD8^+$ CTL (**B**), B cells (**C**), and macrophages (**D**) from secondary lymphoid tissues (spleen, axillary, inguinal, para-aortic, and mesenteric lymph nodes) at the peak of EAE ($n = 6$). **E** Daily clinical EAE scores. Arrows indicate different phases (blue, early; orange, onset; red, peak; green, recovery) of the disease ($n = 12$). **F** The disease phases (early, onset, peak, and recovery) assessed according to clinical scores. The proportion of TREM-2^+CD4^+ T cells increased in the spleen at two stages of EAE ($n = 6$). **G** The correlation ($R^2 = 0.8729$) between the percentages of TREM-2^+CD4^+ T cells and clinical scores ($n = 38$). **H** The proportions and numbers of TREM-2^+CD4^+ T cells in the brain and spinal cord measured at the peak of EAE ($n = 6$). The data shown are the mean ± SEM. Student's *t*-test was used. $^*P < 0.05$, $^{**}P < 0.01$, $^{***}P < 0.001$, ns, not significantly different. Th, T helper; CFA, complete Freund's adjuvant group; EAE, experimental autoimmune encephalomyelitis

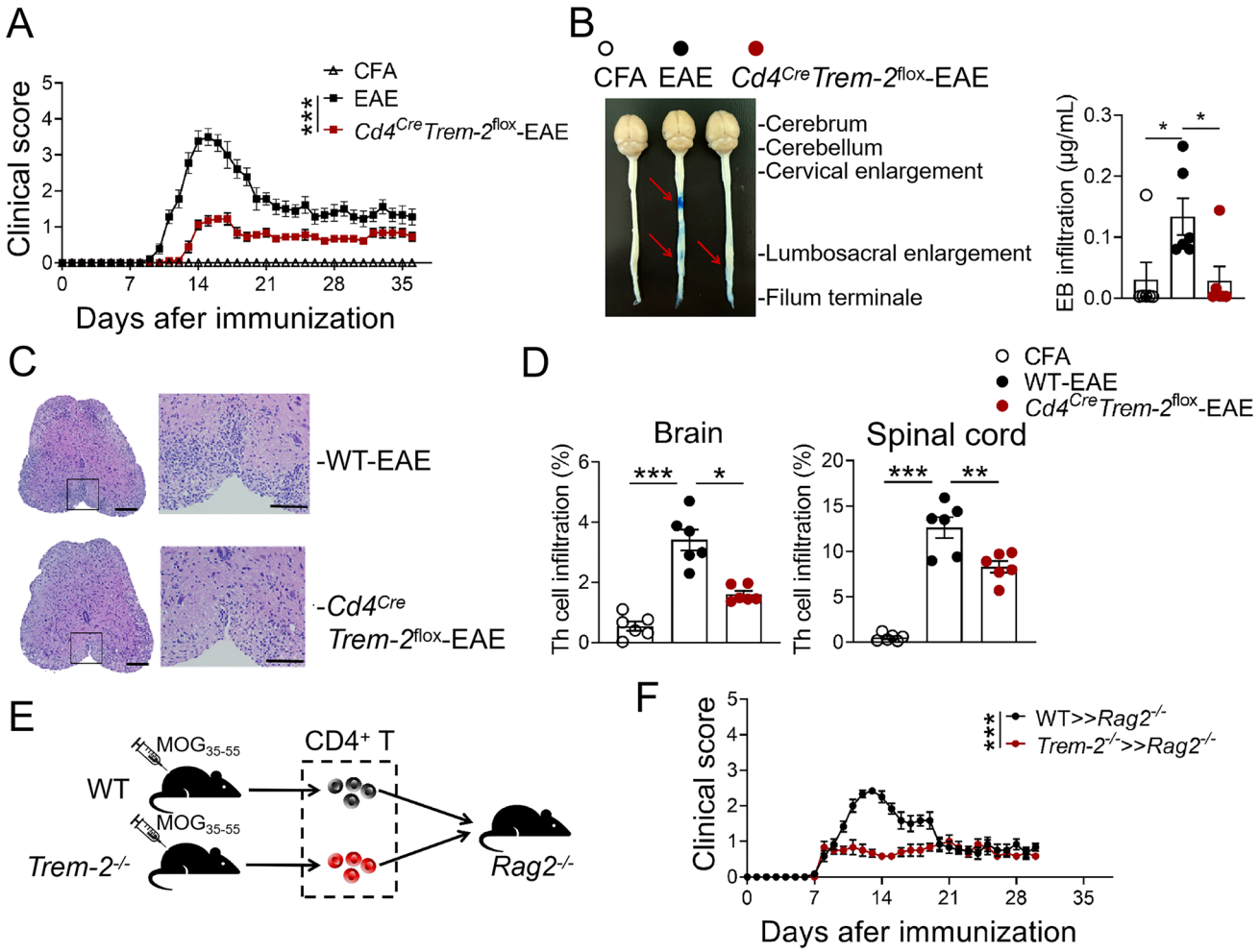

Fig. 3 Conditional knockout of *Trem-2* in CD4$^+$ T cells reduces Th cell infiltration and EAE severity. **A** Daily clinical scores after EAE induction in WT and *Cd4^{Cre}Trem-2^{flox}* mice (n = 6). **B** At the peak of WT-EAE (day 14), EB was injected through the tail vein. After 8 h, brain and spinal cord (CNS) EB concentrations from CFA WT-EAE and *Cd4^{Cre}Trem-2^{flox}*-EAE animals were measured (n = 6). **C** H&E staining of spinal cord sections from WT and *Trem-2$^{-/-}$* mice at the peak of EAE. Scale bars: 200 mm in left images, 50 mm in insets. **D** The proportion of Th cells (CD3$^+$CD4$^+$) gated in CD45$^+$ immune cells infiltrated into the CNS (n = 12). **E** Purified CD4$^+$ T cells from WT-EAE or *Trem-2$^{-/-}$*-EAE mice adoptively transferred into *Rag2$^{-/-}$* mice. **F** Mean clinical EAE scores in immunized WT>>*Rag2$^{-/-}$* or *Trem-2$^{-/-}$>>Rag2$^{-/-}$* mice (n = 6). One-way ANOVA was used. The data shown are the mean ± SEM. *P <0.05, **P <0.01, ***P <0.001

different cell populations were: (1) Naïve (CD4$^+$CD62L$^+$) in B6.2d2 mice; (2) Th17 differentiation from naïve T cells *in vitro* under the $MOG_{35–55}$ peptide (12.5 mg/mL), TGF-β (3 ng/mL), IL-6 (20 ng/mL), and IL-23 (20 ng/mL) (Th17-*vitro*); (3) Adoptive transfer EAE was induced by injecting these *in vitro*-primed Th17 cells into lymphopenic *Rag2$^{-/-}$* mice. At the peak of EAE, Th17 cells were isolated from these mice (Th17-act); (4) After EAE induction with $MOG_{35–55,}$ CD4$^+$ T cells were isolated at the peak of EAE (Th-*vivo*). The design of experimental sample collection for these data is shown in Fig. 4A. Compared with Naïve T cells, TREM-2 was strongly expressed in Th17 cells (Fig. 4B, n = 3, Naïve T *vs* Th-*vivo*: P = 0.002; Naïve T *vs* Th17-*vitro*: P = 0.012; Naïve T *vs* Th17-act: P = 0.02; Th17-*vitro* *vs* Th17-act: P <0.001). Other TREMs did not significantly change during Th17 activation and polarization. As a key cytokine of Th17, IL-17 was significantly increased in the serum of EAE mice at the peak of EAE (Fig. 4C, n = 6, P <0.001). Besides, the increasing concentration of IL-17 was positively correlated with the proportion of TREM-2$^+$CD4$^+$ T cells (Fig. 4D, n = 12, R^2 = 0.674, P = 0.001). The levels of the Th17-related factors IL-6, TNF-α, and IFN-γ, but not IL-23, were increased in the spleen of EAE mice (Fig. 4E, n = 9, IL-6: P <0.001; IL-23: P = 0.052; TNF-α: P <0.001; IFN-γ: P <0.001) and positively correlated with TREM-2$^+$ Th cells (Fig. 4F, n = 18, IL-6: R^2 = 0.8161, P <0.001; IL-23: R^2 = 0.1886, P = 0.072; TNF-α: R^2 = 0.8346, P <0.001; IFN-γ: R^2 = 0.8346, P <0.001) .

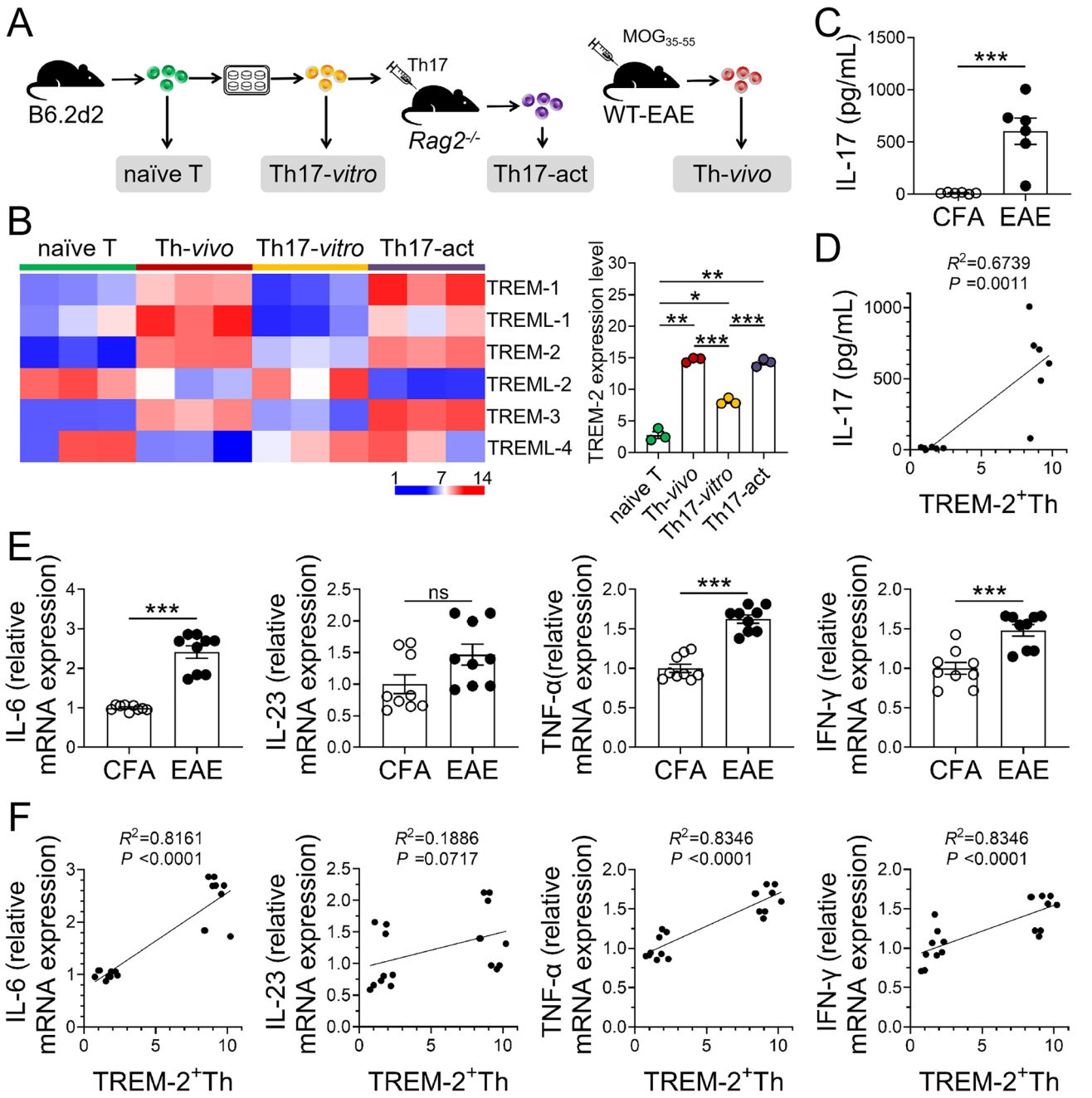

Fig. 4 TREM-2 is positively correlated with Th17 cell differentiation in the EAE model. **A** Experimental design of cells examined for RNA-sequencing. Naïve T cells ($CD4^+CD62L^+$) are isolated from B6.2d2 mice and cultured under Th17-stimulating conditions. For EAE induction, these Th17 cells are injected into *Rag2*$^{-/-}$ mice. At the peak of the disease, Th17-act is collected. Samples for mRNA-sequencing are Naïve T cells, Th17-*vitro*, Th17-act, and Th-*vivo*. **B** Heatmap of mRNA expression of TREM family members (TREM-1, TREML-1, TREM-2, TREML-2, TREM-3, and TREML-4) (n = 3). Red means relatively up-regulated genes and blue means relatively down-regulated genes. **C** IL-17 secretion in serum as evaluated by ELISA at the peak of EAE (n = 6). **D** Pearson's R correlation between the percentage of TREM-2^+CD4^+ cells and the concentration of IL-17 (n = 12, R^2 = 0.6739). **E** qPCR of the expression of cytokines (IL-6, IL-23, TNF-α, and IFN-γ) (n = 9). **F** Correlation analysis between TREM-2^+CD4^+ cells and the cytokines (n = 18) (IL-6: R^2 = 0.8161; IL-23: R^2 = 0.1886; TNF-α: R^2 = 0.8346; IFN-γ: R^2 = 0.8346). *T*-test and one-way ANOVA were used. The data shown are the mean ± SEM. **P* <0.05, ***P* <0.01, ****P* <0.001

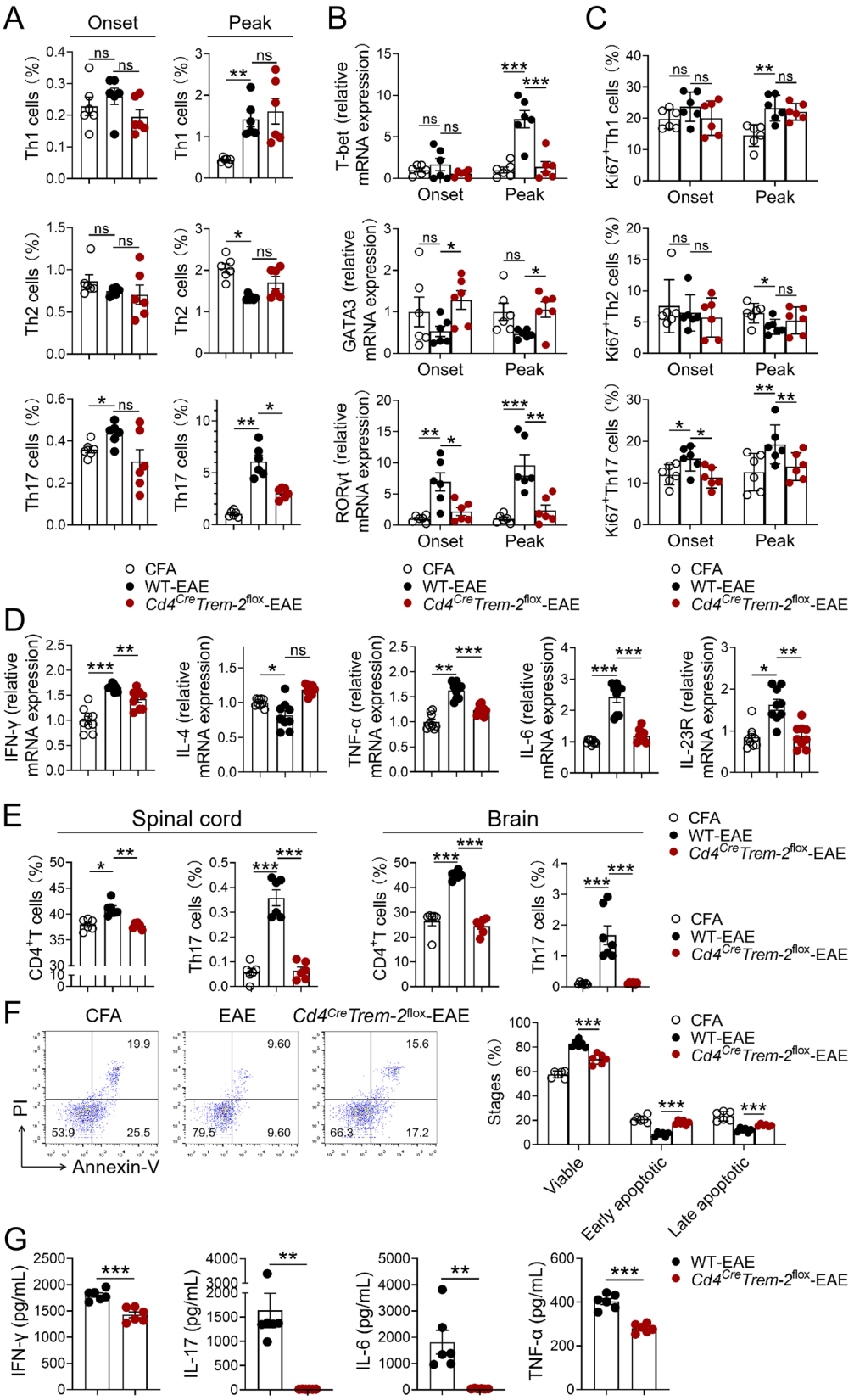
A
Onset
Peak
Th1 cells (%)
Th2 cells (%)
Th17 cells (%)
B
T-bet (relative mRNA expression)
GATA3 (relative mRNA expression)
RORγt (relative mRNA expression)
C
Ki67+Th1 cells (%)
Ki67+Th2 cells (%)
Ki67+Th17 cells (%)
CFA
WT-EAE
Cd4CreTrem-2flox-EAE
D
IFN-γ (relative mRNA expression)
IL-4 (relative mRNA expression)
TNF-α (relative mRNA expression)
IL-6 (relative mRNA expression)
IL-23R (relative mRNA expression)
E
Spinal cord
Brain
CD4+T cells (%)
Th17 cells (%)
F
CFA
EAE
Cd4CreTrem-2flox-EAE
PI
Annexin-V
19.9
53.9
25.5
9.60
79.5
9.60
15.6
66.3
17.2
Stages (%)
Viable
Early apoptotic
Late apoptotic
G
IFN-γ (pg/mL)
IL-17 (pg/mL)
IL-6 (pg/mL)
TNF-α (pg/mL)

◂**Fig. 5** TREM-2 promotes EAE development by regulating Th17 cells. **A** Flow cytometry showing the proportions of Th1, Th2, and Th17 cells at the onset and peak stages of WT-EAE ($n = 6$). **B** The expression of transcription factors of Th cells as measured by qPCR ($n = 6$). **C** The proportion of Ki67-positive Th cells as measured by flow cytometry ($n = 6$). **D** The expression of Th-related cytokines as measured by qPCR ($n = 9$). **E** The proportion of $CD4^+$ T cells (gated in lymphocytes) and Th17 cells (gated in $CD4^+$ T cells) as measured by flow cytometry ($n = 6$) in the spinal cord and brain. **F** The apoptosis of splenic cells after stimulation with $MOG_{35–55}$ for 48 h ($n = 6$). **G** The cytokine concentration in the culture supernatant as measured by ELISA ($n = 6$). *T*-test and one-way ANOVA were used. The data shown are the mean ± SEM. **P* <0.05, ***P* <0.01, ****P* <0.001

These results indicated that TREM-2 is correlated with Th17 differentiation during EAE.

Then, to determine whether TREM-2 promotes Th17 cells in the onset and the peak stages of EAE, the proportion of $CD4^+$ T subsets (Th1, Th2, and Th17) from CFA, WT-EAE, and $Cd4^{Cre}Trem\text{-}2^{flox}$-EAE mice were monitored by flow cytometry (Fig. 5A). Compared with the WT-EAE group, Th17 but not Th1 or Th2 cells were reduced in the spleen of $Cd4^{Cre}Trem\text{-}2^{flox}$-EAE mice in the peak stage of EAE (Fig. 5A, $n = 6$, $P = 0.035$). The expression of important transcription factors, including T-bet (Th1), GATA3 (Th2), and retinoid-related orphan receptor-γt (RORγt) (Th17), were also tested. The results showed that in both onset and peak stages of EAE, *Trem-2* knockout suppressed expression of the transcription factor RORγt, but had no effect on T-bet and GATA3 (Fig. 5B, $n = 6$, Onset RORγt: $P = 0.014$; Peak RORγt: $P = 0.004$). Besides, at the peak of EAE, *Trem-2* knockout also decreased the number of proliferated ($Ki67^+$) Th17 cells (activated Th17 cells) (Fig. 5C, $n = 6$, Onset $Ki67^+$Th17: $P = 0.030$; Peak $Ki67^+$Th17: $P = 0.004$). Furthermore, Th1 and Th17-related cytokines, such as IFN-γ, TNF-α, IL-23, and IL-6, were decreased in the spleen of the $Cd4^{Cre}Trem\text{-}2^{flox}$-EAE group compared with those of the WT-EAE group (Fig. 5D, $n = 9$, IFN-γ WT-EAE *vs* $Cd4^{Cre}Trem\text{-}2^{flox}$-EAE: $P = 0.003$; TNF-α WT-EAE *vs* $Cd4^{Cre}Trem\text{-}2^{flox}$-EAE: $P < 0.001$; IL-6 WT-EAE *vs* $Cd4^{Cre}Trem\text{-}2^{flox}$-EAE: $P < 0.001$; IL-23R WT-EAE *vs* $Cd4^{Cre}Trem\text{-}2^{flox}$-EAE: $P = 0.003$). These results indicated that *Trem-2* knockout affects the proportion of Th17 cells and the production of cytokines. In the CNS of EAE mice, *Trem-2* knockout also decreased the proportion of $CD4^+$ T cells and Th17 cells (Fig. 5E, $n = 6$, spinal cord $CD4^+$ T: $P = 0.005$; spinal cord Th17: $P < 0.001$; brain $CD4^+$ T: $P < 0.001$; brain Th17 cells: $P < 0.001$). *In vitro*, $MOG_{35–55}$, as antigen stimulation, was used to test the antigen-specific $CD4^+$ T cell response. After stimulation for 48 h, the apoptotic rate of $Cd4^{Cre}Trem\text{-}2^{flox}$ T cells was significantly higher than that of the WT-EAE group (Fig. 5F, $n = 6$, $P < 0.001$). Moreover, the Th17-related cytokines IFN-γ, TNF-α, IL-17, and IL-6 levels were reduced in TREM-2-deficient T cells (Fig. 5G, $n = 6$, IFN-γ: $P < 0.001$; IL-17: $P = 0.001$; IL-6: $P = <0.001$; TNF-α: $P < 0.001$). These results demonstrated that TREM-2 promotes EAE progression by inducing Th17 cells.

TREM-2 Promotes the Differentiation and Function of Th17 Cells in EAE

Th17 cells are differentiated from naïve $CD4^+$ T cells exposed to a specific cytokine environment, including IL-6, IL-21, and IL-23R. The Th17 response is enhanced by IL-17, TNF-α, and IFN-γ but suppressed by IL-10 [39]. Besides, Th17 cells also express GM-CSF to promote immune responses to self-antigens [40–42]. To further evaluate the direct role of TREM-2 engagement on $CD4^+$ T cells in the development of EAE, the passive transfer model of EAE disease was used (Fig. 6A). We found that $Rag2^{-/-}$ mice that received $CD4^+$ T cells transferred from $Trem\text{-}2^{-/-}$ mice showed impaired pathology upon EAE induction (Fig. 6B, $n = 6$, $P < 0.001$). In addition, we found that fewer $CD4^+$ T cells accumulated in the lymph nodes and spleen of the $Rag2^{-/-}$ mice reconstituted with $Trem\text{-}2^{-/-}$ $CD4^+$ T cells compared with those with WT $CD4^+$ T cells [Fig. 6C, $n = 6$, MLN: $P = 0.08$; spleen (SP) : $P < 0.001$], and $Trem\text{-}2^{-/-}$ $CD4^+$ T cells exhibited a less activated phenotype (Fig. 6D, $n = 6$). In the peak stage, IL-17, IL-6, TNF-α, and IFN-γ were reduced in the serum from $Rag2^{-/-}$ mice -EAE reconstituted with $Trem\text{-}2^{-/-}$ $CD4^+$ T cell ($Trem\text{-}2^{-/-}$>>$Rag2^{-/-}$) compared to those from $Rag2^{-/-}$ mice -EAE reconstituted with WT $CD4^+$ T cells (WT>>$Rag2^{-/-}$) (Fig. 6E, F; $n = 6$, IL-17: $P = 0.07$, IL-6: $P = 0.036$, TNF-a: $P = 0.024$, IFN-r: $P = 0.034$). RORγt, an important transcription factor of Th17 differentiation and function, and Th17-related cytokines were reduced in the $Trem\text{-}2^{-/-}$ group (Fig. 6E–H, $n = 6$, IL-22: $P = 0.002$; IL-23R: $P < 0.001$; RORγt: $P < 0.001$; GM-CSF: $P < 0.001$). In summary, our data implicated TREM-2 as essential for the differentiation and functional phases of Th17 cells in EAE.

TREM-2 Promotes the Pro-inflammatory Function of Th17 Through pZAP70/STAT3

Our previous studies suggested that TREM-2 promotes Th1 responses by interacting with the CD3ζ/ZAP70 complex following infection with *M. tuberculosis* and SARS-CoV-2 [27, 28]. To investigate the role of TREM-2-mediated CD3ζ/ZAP70 signaling in Th17 differentiation during EAE development, we reanalyzed this gene signature in the database (GSE57098) of Naïve T and Th17 cells. The results showed that the genes encoding TNF-α, IL-6, IL-17, and GM-CSF were highly expressed on Th17 cells (Fig. 7A), which is consistent with the previous report [43]. Furthermore, STAT3 was also found to be highly expressed in Th17 cells (Fig. 7A, $n = 3$, Naïve T *vs* Th-*vivo*: $P = 0.001$; Naïve T *vs* Th17-*vitro*:

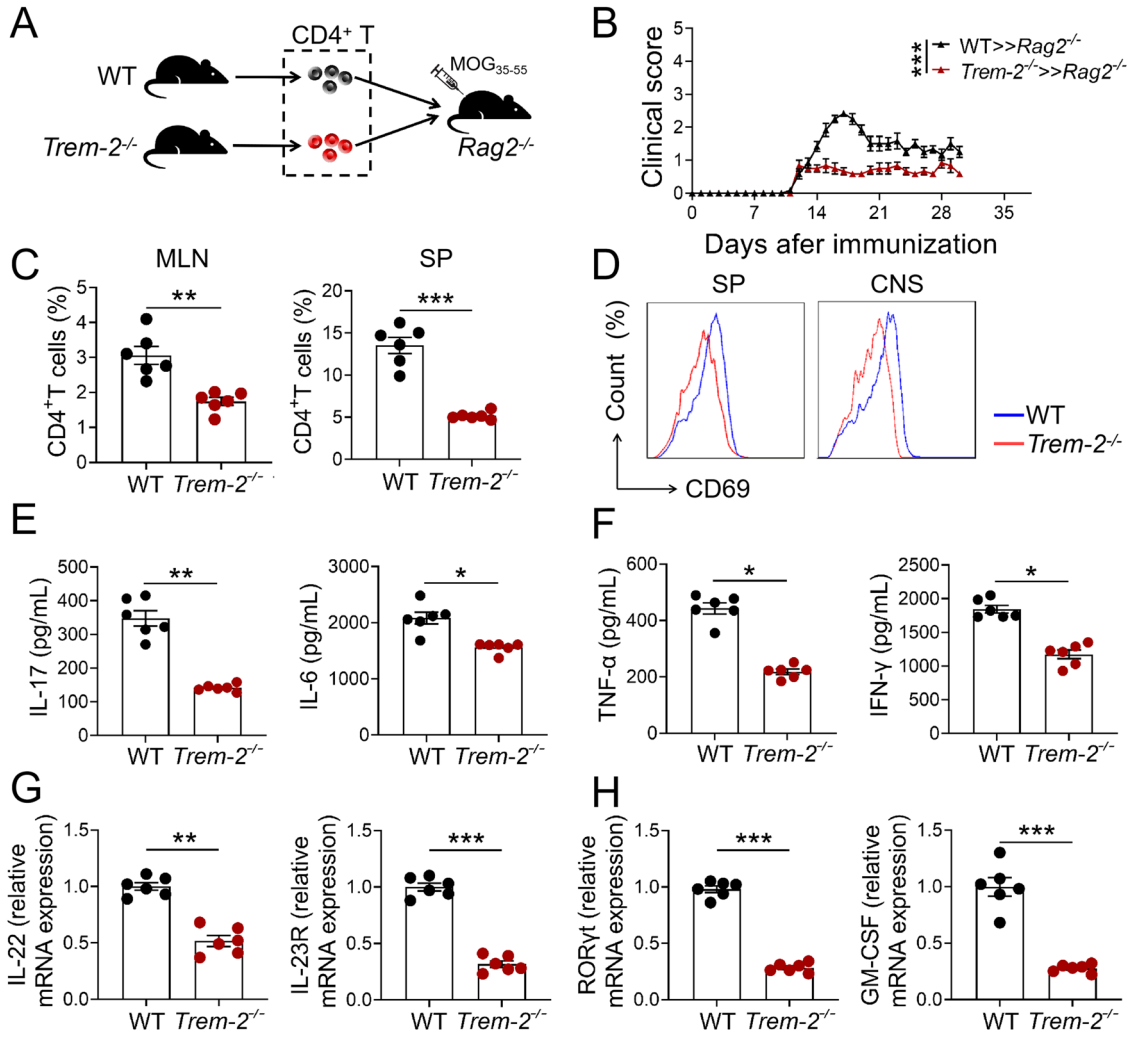

Fig. 6 TREM-2 promotes Th17 cell differentiation, proliferation, and cytokine secretion in EAE. **A** *Rag2*$^{-/-}$ mice are reconstituted with WT or TREM-2-deficient CD4$^+$ T cells. and EAE is induced (n = 6). **B** Clinical scores (n = 6). **C** The frequency of CD4$^+$ T cells from lymph nodes and spleen (n = 6). **D** The expression of the activation marker CD69 on splenic CD4$^+$ T cells (n = 6). **E, F** Concentrations of IL-17, IL-6, TNF-a, and IFN-γ in serum as measured by ELISA (n = 6) at the peak of EAE. **G, H** The mRNA expression of IL-22, IL-23R, RORγt, and GM-CSF as measured by qPCR (n = 6). *T*-test was used. The data shown are the mean ± SEM. **P* <0.05, ***P* <0.01, ****P* <0.001

$P = 0.022$; Naïve T *vs* Th17-act: $P = 0.020$). However, there was no significant difference in ZAP70 expression between Naïve T and Th17 cells (Fig. 7A). As an essential kinase in T cell signaling, only phosphorylated ZAP70 (pZAP70) could regulate STAT3 [44]. The proportions of STAT3-, pZAP70-, TNF-α-, and IL-6-positive cells among Th17 cells were increased in the EAE model compared with the CFA group (Fig. 7B, $n = 6$, STAT3$^+$Th17: $P = 0.004$; pZAP70$^+$Th17: $P = 0.007$; TNF-α$^+$Th17: $P = 0.006$; IL-6$^+$Th17: $P = 0.026$). We found that these factors were decreased in Th17 cells from the *Cd4*^{Cre}*Trem-2*^{flox}-EAE group compared to the WT-EAE group (Fig. 7B, $n = 6$, STAT3$^+$Th17: $P = 0.013$; pZAP70$^+$Th17: $P = 0.013$; TNF-α$^+$Th17; $P = 0.006$; IL-6$^+$Th17: P <0.001). Next, to test whether the proportion of Th17 (IL-17A$^+$ CD4$^+$) cells is affected by pZAP70 or STAT3 or both, we analyzed the expression of IL-17A$^+$ or IL-6$^+$Th17 in TREM-2-, pZAP70-, or STAT3-positive CD4$^+$ T cells. Co-expression of TREM-2, STAT3, and pZAP70 induced IL-17 production in CD4$^+$ T cells (Fig. 7C, $n = 6$, TREM-2$^+$pZAP70$^+$STAT3$^+$ *vs* others: P <0.001). STAT3$^-$ or pZAP70$^-$ or TREM-2$^-$ Th cells expressed relatively low levels of IL-17A (Fig. 7C). The expression of IL-6 on Th17 cells was also affected by TREM-2, pZAP70, and STAT3 (Fig. 7D, $n = 6$, TREM-2$^+$pZAP70$^+$STAT3$^+$ *vs* TREM-2$^+$pZAP70$^-$STAT3$^-$: P <0.001; TREM-2$^+$pZAP70$^+$STAT3$^+$ *vs* TREM-2$^-$pZAP70$^+$STAT3$^+$: P = 0.004). *In vivo* experiments showed that the proportion of Th17 and their ability to secrete IL-6 were both reliant on

TREM-2, pZAP70, and STAT3. For *in vitro* experiments, MOG_{35-55} was used to culture mouse spleen cells. With MOG_{35-55} re-stimulation, the levels of pSTAT3 and pZAP70 on $CD4^+$ T cells were increased in WT-EAE mice while decreased in $Cd4^{Cre}Trem\text{-}2^{flox}$-EAE mice (Fig. 7E). In addition, TREM-2 deficiency in $CD4^+$ T cells suppressed the secretion of IL-6 and IL-17 (Fig. 7F, $n = 6$, WT-EAE *vs* $Cd4^{Cre}Trem\text{-}2^{flox}$-EAE IL-17: $P = 0.002$; IL-6: $P < 0.001$) and the expression of GM-CSF, TNF-α, and IFN-γ (Fig. 7G, $n = 6$, WT-EAE *vs* $Cd4^{Cre}Trem\text{-}2^{flox}$-EAE GM-CSF: $P < 0.001$; TNF-α: $P < 0.001$; STAT3: $P < 0.001$; IFN-γ: $P < 0.001$). Pre-treatment with the ZAP70 inhibitor 4-amino-5-(4-chlorophenyl)-7-(t-butyl) pyrazolo(3,4-d)pyrimidine (phloem protein 2, PP2), reduced these cytokines in the WT-EAE group (Fig. 7F, G; $n = 6$; WT-EAE *vs* WT-EAE+PP2 IL-17: $P = 0.039$; IL-6: $P = 0.007$; GM-CSF: $P < 0.001$; TNF-a: $P = 0.005$; STAT3: $P < 0.001$; IFN-γ: $P < 0.001$). And there was no significant difference between the WT-EAE and $Cd4^{Cre}Trem\text{-}2^{flox}$-EAE groups upon PP2 treatment. These data indicated that TREM-2 affects the secretion of IL-6 and IL-17 and the expression of GM-CSF, TNF-α, and IFN-γ through pZAP70/STAT3.

Discussion

MS, a chronic inflammatory, demyelinating, and neurodegenerative disease, cannot be cured [45]. The clinical observations indicate that a therapeutic effect is related to the fluctuation of Th17 cell proportion and function [46]. Th17 is considered a pathogenic factor of MS and an important target to cure patients. Based on this proposal, we aimed to investigate a key regulatory mechanism of Th17 in MS.

First, we showed a difference in peripheral $CD4^+$ T cells between patients with MS and healthy people by analyzing their mRNA-sequencing data. The data from flow cytometry also showed that peripheral $CD4^+$ T cells from patients with MS expressed high levels of Th17-related cytokines (IL-17, TNF, GM-CSF, and IFN-γ) which is consistent with the previous reports [47]. Importantly, TREM-2 was identified to be highly expressed by Th17 cells from patients with MS. As a pattern recognition receptor, TREM-2 has been reported to regulate Th differentiation [28]. Moreover, TREM-2 has a structural basis as a regulatory molecule interacting with antigen-presenting cells and T cells [23, 24]. We hypothesized that TREM-2 might be the receptor that regulates peripheral Th17 in MS.

In order to assess the expression level of TREM-2, we established the EAE-mouse model, which is the most commonly-used experimental model for MS. During EAE, TREM-2^+CD4^+ T cells were increased in the spleen and positively correlated with the clinical score. TREM-2 was also expressed on CTL cells, B cells, and macrophages. However, the TREM-2 expression level of these immune cells did not have a significant relationship with EAE. Therefore, we generated $Cd4^{Cre}Trem\text{-}2^{flox}$ mice to further verify the specific role of TREM-2 on $CD4^+$ T cells during EAE. The clinical score, BBB permeability, and immune cell infiltration, which are characteristic of MS [48], were decreased in $Cd4^{Cre}Trem\text{-}2^{flox}$-EAE mice. The normal BBB effectively prevents EB from entering the central nervous system from the blood circulation, so EB was used to assess BBB permeability [49]. In our study, $Cd4^{Cre}Trem\text{-}2^{flox}$ mice were protected against immunization-induced autoimmune neuroinflammation and this result is consistent with the previous reports [33]. Based on the literature and our results, we believe that three reasons contribute to this phenomenon. First, here, we used *Trem-2* knockout mice to explore the effect of TREM-2 on EAE, while Laura Piccio *et al.* used TREM-2 blocking antibody, which may lead to the diversity of the intervening effect. Secondly, TREM-2 plays various roles in different cells *via* different mechanisms, so it may play different roles in different stages of EAE. In the discussion section of reference 33, the authors mention that the exacerbating effect of blocking TREM-2 only works before the clinical onset of EAE (days 5 and 9). This means that TREM-2 plays different roles in different stages of EAE. Most of the previous reports on TREM-2, including reference 33, mainly focus on the function of TREM-2/DAP12 in myeloid cells [29, 30]. In fact, TREM-2 could initiate distinct downstream signaling pathways in different immune cells. We found here that TREM-2 played a regulatory role in EAE *via* affecting Th17 cells, and it has been demonstrated that the CD3ζ/ZAP70 signal is the dominant signal pathway downstream of TREM-2 in T cells [27, 28]. Given the complex immune environment in EAE and the complicated signal transduction mediated by TREM-2, it is reasonable to conclude that TREM-2 plays diverse roles during EAE by affecting the outcomes of different immune cells. Meanwhile, $Rag2^{-/-}$ mice reconstituted with $Trem\text{-}2^{-/-}$ $CD4^+$ T cells developed decreased EAE disease. These results demonstrated that TREM-2 is an essential factor for the pathogenicity of $CD4^+$ T cells in EAE. By analyzing the mRNA expression profiles of Naïve T and Th17 cells, we found that TREM-2 was highly expressed in activated Th17 cells in EAE. Interestingly, Th17 extracted directly from EAE mice (Th17-act) had the highest levels of TREM-2 expression. These data indicated that TREM-2 might be a biomarker for the diagnosis and auxiliary monitoring of EAE. As in previous studies [50], the secretion of IL-17, IL-6, TNF-α, and IFN-γ was higher in EAE. These Th17-related cytokines are all strongly correlated with the proportion of TREM-2^+CD4^+ T cells. However, IL-23 did not increase in EAE $CD4^+$ T cells. Two possible reasons may be as follows. Firstly, IL-23 may have played an important role in the generation of encephalitogenic cells during the

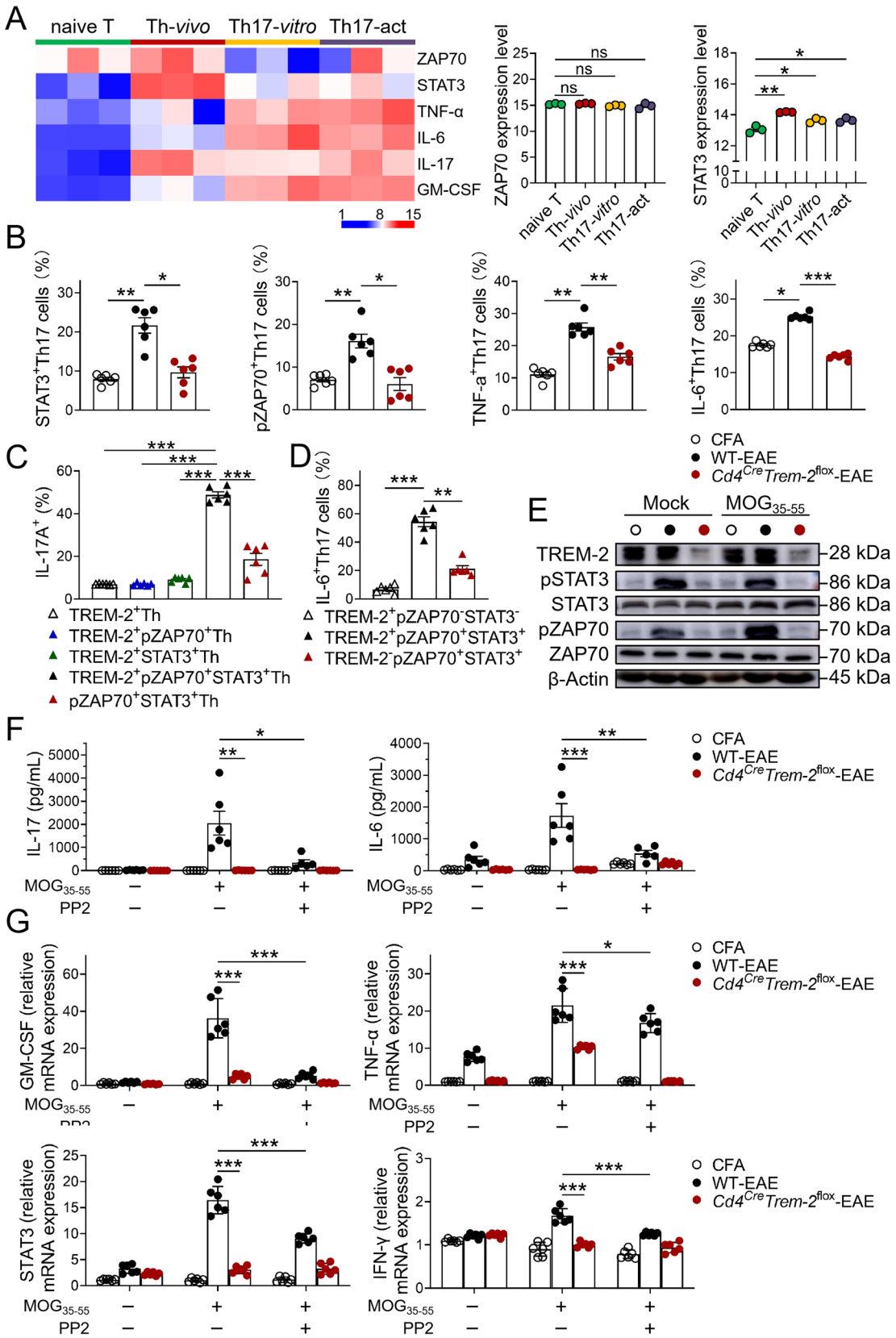
A
naive T
Th-vivo
Th17-vitro
Th17-act
ZAP70
STAT3
TNF-α
IL-6
IL-17
GM-CSF
1 8 15
ZAP70 expression level
STAT3 expression level
ns
B
STAT3+Th17 cells (%)
pZAP70+Th17 cells (%)
TNF-a+Th17 cells (%)
IL-6+Th17 cells (%)
C
IL-17A+ (%)
TREM-2+Th
TREM-2+pZAP70+Th
TREM-2+STAT3+Th
TREM-2+pZAP70+STAT3+Th
pZAP70+STAT3+Th
D
IL-6+Th17 cells (%)
TREM-2+pZAP70-STAT3-
TREM-2+pZAP70+STAT3+
TREM-2-pZAP70+STAT3+
CFA
WT-EAE
Cd4CreTrem-2flox-EAE
E
Mock
MOG35-55
TREM-2
pSTAT3
STAT3
pZAP70
ZAP70
β-Actin
28 kDa
86 kDa
86 kDa
70 kDa
70 kDa
45 kDa
F
IL-17 (pg/mL)
IL-6 (pg/mL)
MOG35-55
PP2
G
GM-CSF (relative mRNA expression)
TNF-α (relative mRNA expression)
STAT3 (relative mRNA expression)
IFN-γ (relative mRNA expression)

◂**Fig. 7** TREM-2 promotes pathogenic Th17 *via* the pZAP70/STAT3 pathway in EAE. **A** Heatmap of the expression of ZAP70, STAT3, and related cytokines ($n = 3$). Red means relatively up-regulated genes, and blue means relatively down-regulated genes. **B** STAT3, phosphorylated-ZAP70 (pZAP70), TNF-α, and IL-6 levels in Th17 cells as detected by flow cytometry ($n = 6$). **C, D** The percentages of IL-17a$^+$ and IL-6$^+$ Th17 measured in Th cells in the absence or presence of pZAP70, STAT3, or TREM-2 ($n = 6$). **E**, Western blots of the levels of phosphorylated and total STAT3 and ZAP70 with $MOG_{35–55}$ incubation. **F, G** Purified WT and TREM-2 deficient CD4$^+$ T cells from spleens stimulated with $MOG_{35–55}$ in the presence or absence of the pZAP70 inhibitor PP2 (20 ng/mL). The levels of IL-6 and IL-17 secretion as detected by ELISA ($n = 6$). The mRNA expression of GM-CSF, TNF-α, STAT3, and IFN-γ as determined by qPCR ($n = 6$). One-way ANOVA was used. The data shown are the mean ± SEM. *P <0.05, **P <0.01, ***P <0.001

induction phase of EAE, not in the effector phase [51]. Secondly, IL-23 may have been produced by antigen-presenting cells, such as dendritic cells and monocytes/macrophages. Here, we analyzed the gene expression in CD4$^+$ T cells. It has been reported that IL-23 binds to the IL-23R on CD4$^+$ T cells, which promotes the expression of IL-17 *via* STAT3 [52, 53]. Based on the relationship between TREM-2 and Th17, we hypothesized that TREM-2 may promote EAE progression by affecting Th17 cells and so we assessed the proportions and related cytokines of Th1, Th2, and Th17 cells in CFA, WT-EAE, and *Cd4*^{Cre}*Trem-2*^{flox}-EAE mice. Our results showed that *Trem-2* knockout decreased the activation, proliferation, and differentiation of Th17 cells as well as the expression of TNF-α, IFN-γ, IL-6, and IL-23R. *In vitro,* after $MOG_{35–55}$ stimulation, the proportion of viable cells and secretion of TNF-α, IFN-γ, and IL-6 were also decreased with *Trem-2* knockout. These results confirmed that TREM-2 is essential for Th17 cell pathogenesis in EAE.

As drivers and the main culprits of autoimmune response, the pathogenicity of Th17 cells is influenced in three aspects: their polarization, maintenance (expansion), and cytokine secretion [50]. During initial Th17 development, IL-6 and IL-21 promote the early activation of CD4$^+$ T cells, which then acts as a positive amplification loop to enforce Th17 differentiation [54]. In the initial stage, STAT3 is activated and induces the secretion of IL-6 and IL-17 [53]. In work by others, it has also been reported that the absence of IL-21 or IL-21R has no significant effect on Th17 differentiation [55, 56]. We found

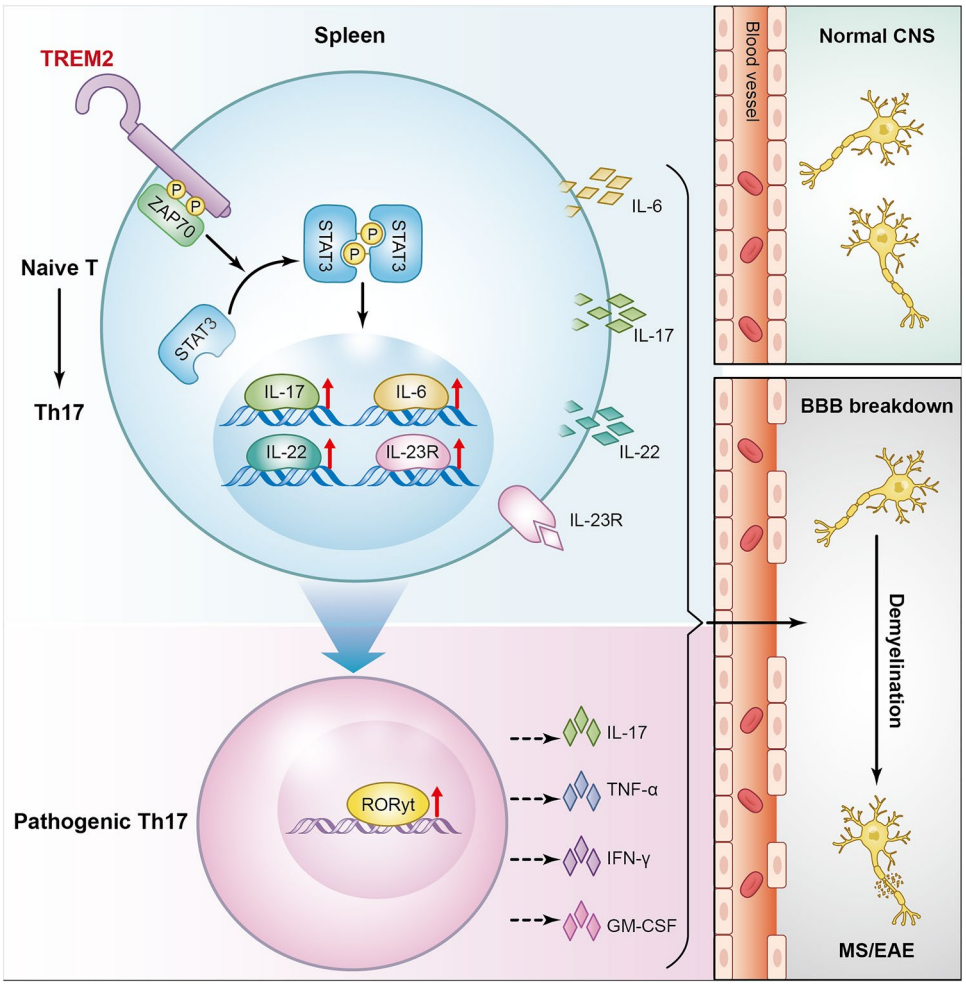

Fig. 8 Graphical abstract. In patients with MS and the EAE model, TREM-2 is up-regulated in CD4$^+$ T cells and activates the phosphorylation of ZAP70 and STAT3 in CD4$^+$ T cells, which is essential for Th17 differentiation. In the initial phase, TREM-2 promotes Th17 differentiation by enhancing IL-6, IL-17, IL-22, and IL-23R expression. In the effective stage, TREM-2 induces the pathogenic polarization of Th17 cells, which secrete IL-17, TNF-α, IFN-γ, and GM-CSF. TREM-2-mediated Th17 activation and polarization result in BBB damage and neuroinflammation.

that TREM-2 induced the expression of IL-6, IL-22, and IL-23R in $CD4^+$ T cells. IL-23 is also essential for the maintenance and expansion (not initiation) of pathogenic Th17 cells but not naïve T cells with low IL23R [57]. Th17 differentiation is finally stabilized along with the up-regulation of IL-23R [58]. During the maintenance and expansion stage, retinoic acid receptor-related orphan RORγt, IL-17, IL-22, and GM-CSF are also enhanced [47]. In our study, the expression of IL-23R and RORγt were used to assess the stability of pathogenic Th17 in the differentiation and expansion stages. Autoreactive Th17 cells also secrete IL-17, IL-6, IL-21, IL-22, GM-CSF, TNF-α, and IFN-γ, which have proinflammatory actions to promote the neuroinflammatory reaction of MS [50]. BBB disruption, an early and central event in MS pathogenesis, is caused by IL-17 and IL-22, which disrupt tight junction proteins in the CNS endothelial cells [59]. In our study, *Rag2*$^{-/-}$ mice reconstituted with *Trem-2*$^{-/-}$ $CD4^+$ T cells (*Trem-2*$^{-/-}$>>*Rag2*$^{-/-}$ group) exhibited decreases in EAE disease severity, lower numbers and activity of $CD4^+$ T cells, and lower expression of cytokines (IL-17, IL-6, IL-22, IL-23R, TNF-α, IFN-γ, RORγt, and GM-CSF). Furthermore, TREM-2 did not affect the early T cell development and maturation. Taken together, we concluded that TREM-2 is an essential factor during the differentiation and functional phases of Th17 cells.

Our previous studies have found that TREM-2 interacts with the TCR-CD3ζ-ZAP70 complex and enhances proinflammatory Th1 responses [27]. As a cytoplasmic tyrosine phosphoprotein, ZAP70 has been reported to play important roles in modulating the leukemia inhibitory factor (LIF)/Janus kinase (JAK)/STAT3 signaling pathway [44]. STAT3 is critical for the differentiation of Th17 from naïve $CD4^+$ T cells [54]. We also found that TREM-2 augmented the production of IL-17, IL-6, GM-CSF, TNF-α, and IFN-γ by enhancing the pZAP70/STAT3 signal in $CD4^+$ T cells.

In summary, we found that TREM-2 regulated $CD4^+$ T cell-mediated autoimmunity *in vivo*, while the loss of TREM-2 in $CD4^+$ T cells dramatically ameliorated EAE development. TREM-2 promoted EAE progression by affecting the differentiation, expansion, and cytokine production of Th17 cells. Furthermore, we demonstrated that TREM-2 engagement on $CD4^+$ T cells regulated the pathogenic Th17 by inducing pZAP70/STAT3 signaling (Fig. 8). This study sheds new light on regulating proinflammatory Th17 and provides potential therapeutic targets for MS.

Acknowledgements This work was supported by grants from the National Natural Science Foundation of China (82072062, 82270016, and 82102249), the National Science and Technology Key Projects for Major Infectious Diseases (2017ZX10302301-002), the Natural Science Foundation of Guangdong Province (2023A1515030065), the Open Research Funds from the Sixth Affiliated Hospital of Guangzhou Medical University, Qingyuan People's Hospital (202301-102), and the Development Project of Foshan Fourth People's Hospital (FSSYKF-2020003).

Conflict of interest The authors declare that there are no conflicts of interest.

References

1. Kamińska J, Koper OM, Piechal K, Kemona H. Multiple sclerosis - etiology and diagnostic potential. Postepy Hig Med Dosw (Online) 2017, 71: 551–563.
2. Nelke C, Schroeter CB, Pawlitzki M, Meuth SG, Ruck T. Cellular senescence in neuroinflammatory disease: New therapies for old cells? Trends Mol Med 2022, 28: 850–863.
3. Oh J, Bar-Or A. Emerging therapies to target CNS pathophysiology in multiple sclerosis. Nat Rev Neurol 2022, 18: 466–475.
4. Hou H, Sun Y, Miao J, Gao M, Guo L, Song X. Ponesimod modulates the Th1/Th17/Treg cell balance and ameliorates disease in experimental autoimmune encephalomyelitis. J Neuroimmunol 2021, 356: 577583.
5. Li B, Wang X, Choi IY, Wang YC, Liu S, Pham AT. miR-146a modulates autoreactive Th17 cell differentiation and regulates organ-specific autoimmunity. J Clin Invest 2017, 127: 3702–3716.
6. Danikowski KM, Jayaraman S, Prabhakar BS. Regulatory T cells in multiple sclerosis and myasthenia gravis. J Neuroinflammation 2017, 14: 117.
7. Courtney AH, Lo WL, Weiss A. TCR signaling: Mechanisms of initiation and propagation. Trends Biochem Sci 2018, 43: 108–123.
8. Ashe JM, Wiest DL, Abe R, Singer A. ZAP-70 protein promotes tyrosine phosphorylation of T cell receptor signaling motifs (ITAMs) in immature $CD4^+{}_8{}^+$ thymocytes with limiting p56(lck). J Exp Med 1999, 189: 1163–1168.
9. Deindl S, Kadlecek TA, Brdicka T, Cao X, Weiss A, Kuriyan J. Structural basis for the inhibition of tyrosine kinase activity of ZAP-70. Cell 2007, 129: 735–746.
10. Lo WL, Shah NH, Ahsan N, Horkova V, Stepanek O, Salomon AR, *et al*. Lck promotes Zap70-dependent LAT phosphorylation by bridging Zap70 to LAT. Nat Immunol 2018, 19: 733–741.
11. Gaud G, Lesourne R, Love PE. Regulatory mechanisms in T cell receptor signalling. Nat Rev Immunol 2018, 18: 485–497.
12. Lee PW, Smith AJ, Yang Y, Selhorst AJ, Liu Y, Racke MK, *et al*. IL-23R-activated STAT3/STAT4 is essential for Th1/Th17-mediated CNS autoimmunity. JCI Insight 2017, 2: e91663.
13. Wang F, Yang Y, Li Z, Wang Y, Zhang Z, Zhang W, *et al*. Mannan-binding lectin regulates the Th17/treg axis through JAK/STAT and TGF-β/SMAD signaling against *Candida albicans* infection. J Inflamm Res 2022, 15: 1797–1810.
14. Lee JY, Hall JA, Kroehling L, Wu L, Najar T, Nguyen HH, *et al*. Serum amyloid A proteins induce pathogenic Th17 cells and promote inflammatory disease. Cell 2020, 183: 2036–2039.
15. Harbour SN, DiToro DF, Witte SJ, Zindl CL, Gao M, Schoeb TR, *et al*. T_H17 cells require ongoing classic IL-6 receptor signaling to retain transcriptional and functional identity. Sci Immunol 2020, 5: eaaw2262.
16. Yan Z, Yang W, Parkitny L, Gibson SA, Lee KS, Collins F, *et al*. Deficiency of Socs3 leads to brain-targeted EAE via enhanced neutrophil activation and ROS production. JCI Insight 2019, 5: e126520.
17. Xu H, Hiraishi K, Kurahara LH, Nakano-Narusawa Y, Li X, Hu Y, *et al*. Inhibitory effects of breast milk-derived *Lactobacillus rhamnosus* probio-M9 on colitis-associated carcinogenesis by

restoration of the gut microbiota in a mouse model. Nutrients 2021, 13: 1143.
18. Kim NH, Lee SM, Kim YN, Jeon YJ, Heo JD, Jeong EJ, *et al*. Standardized fraction of *Turbinaria ornata* alleviates dextran sulfate sodium-induced chronic colitis in C57BL/6 mice via upregulation of FOXP3+ regulatory T cells. Biomolecules 2020, 10: E1463.
19. Wang D, Huang S, Yuan X, Liang J, Xu R, Yao G, *et al*. The regulation of the Treg/Th17 balance by mesenchymal stem cells in human systemic lupus erythematosus. Cell Mol Immunol 2017, 14: 423–431.
20. Winkelmann A, Loebermann M, Barnett M, Hartung HP, Zettl UK. Vaccination and immunotherapies in neuroimmunological diseases. Nat Rev Neurol 2022, 18: 289–306.
21. Rosciszewski G, Cadena V, Murta V, Lukin J, Villarreal A, Roger T, *et al*. Toll-like receptor 4 (TLR4) and triggering receptor expressed on myeloid cells-2 (TREM-2) activation balance astrocyte polarization into a proinflammatory phenotype. Mol Neurobiol 2018, 55: 3875–3888.
22. Ford JW, McVicar DW. TREM and TREM-like receptors in inflammation and disease. Curr Opin Immunol 2009, 21: 38–46.
23. Sharif O, Gawish R, Warszawska JM, Martins R, Lakovits K, Hladik A, *et al*. The triggering receptor expressed on myeloid cells 2 inhibits complement component 1q effector mechanisms and exerts detrimental effects during pneumococcal pneumonia. PLoS Pathog 2014, 10: e1004167.
24. Daws MR, Sullam PM, Niemi EC, Chen TT, Tchao NK, Seaman WE. Pattern recognition by TREM-2: Binding of anionic ligands. J Immunol 2003, 171: 594–599.
25. Labiano I, Agirre-Lizaso A, Olaizola P, Echebarria A, Huici-Izagirre M, Olaizola I, *et al*. TREM-2 plays a protective role in cholestasis by acting as a negative regulator of inflammation. J Hepatol 2022, 77: 991–1004.
26. Weehuizen TA, Hommes TJ, Lankelma JM, de Jong HK, Roelofs JJ, de Vos AF, *et al*. Triggering receptor expressed on myeloid cells (TREM)-2 impairs host defense in experimental melioidosis. PLoS Negl Trop Dis 2016, 10: e0004747.
27. Wu Y, Wu M, Ming S, Zhan X, Hu S, Li X, *et al*. TREM-2 promotes Th1 responses by interacting with the CD3ζ-ZAP70 complex following Mycobacterium tuberculosis infection. J Clin Invest 2021, 131: e137407.
28. Wu Y, Wang M, Yin H, Ming S, Li X, Jiang G, *et al*. TREM-2 is a sensor and activator of T cell response in SARS-CoV-2 infection. Sci Adv 2021, 7: eabi6802.
29. Jonsson T, Stefansson K. TREM2 and neurodegenerative disease. N Engl J Med 2013, 369: 1564–1570.
30. Jonsson T, Stefansson H, Steinberg S, Jonsdottir I, Jonsson PV, Snaedal J, *et al*. Variant of *TREM2* associated with the risk of Alzheimer's disease. N Engl J Med 2013, 368: 107–116.
31. Chen S, Peng J, Sherchan P, Ma Y, Xiang S, Yan F, *et al*. TREM2 activation attenuates neuroinflammation and neuronal apoptosis via PI3K/Akt pathway after intracerebral hemorrhage in mice. J Neuroinflammation 2020, 17: 168.
32. Zhang J, Zheng Y, Luo Y, Du Y, Zhang X, Fu J. Curcumin inhibits LPS-induced neuroinflammation by promoting microglial M2 polarization via TREM2/TLR4/NF-κB pathways in BV2 cells. Mol Immunol 2019, 116: 29–37.
33. Piccio L, Buonsanti C, Mariani M, Cella M, Gilfillan S, Cross AH, *et al*. Blockade of TREM-2 exacerbates experimental autoimmune encephalomyelitis. Eur J Immunol 2007, 37: 1290–1301.
34. Lampron A, Larochelle A, Laflamme N, Préfontaine P, Plante MM, Sánchez MG, *et al*. Inefficient clearance of myelin debris by microglia impairs remyelinating processes. J Exp Med 2015, 212: 481–495.
35. Chu F, Shi M, Zheng C, Shen D, Zhu J, Zheng X, *et al*. The roles of macrophages and microglia in multiple sclerosis and experimental autoimmune encephalomyelitis. J Neuroimmunol 2018, 318: 1–7.
36. Liu R, Du S, Zhao L, Jain S, Sahay K, Rizvanov A, *et al*. Autoreactive lymphocytes in multiple sclerosis: Pathogenesis and treatment target. Front Immunol 2022, 13: 996469.
37. Yamout Bassem, Alroughani Raed. Multiple Sclerosis. Semin Neurol. 2018, 38: 212–225.
38. Hoppmann N, Graetz C, Paterka M, Poisa-Beiro L, Larochelle C, Hasan M, *et al*. New candidates for CD4 T cell pathogenicity in experimental neuroinflammation and multiple sclerosis. Brain 2015, 138: 902–917.
39. Giles DA, Moreno-Fernandez ME, Stankiewicz TE, Graspeuntner S, Cappelletti M, Wu D, *et al*. Thermoneutral housing exacerbates nonalcoholic fatty liver disease in mice and allows for sex-independent disease modeling. Nat Med 2017, 23: 829–838.
40. Ponomarev ED, Shriver LP, Maresz K, Pedras-Vasconcelos J, Verthelyi D, Dittel BN. GM-CSF production by autoreactive T cells is required for the activation of microglial cells and the onset of experimental autoimmune encephalomyelitis. J Immunol 2007, 178: 39–48.
41. Codarri L, Gyülvészi G, Tosevski V, Hesske L, Fontana A, Magnenat L, *et al*. RORγt drives production of the cytokine GM-CSF in helper T cells, which is essential for the effector phase of autoimmune neuroinflammation. Nat Immunol 2011, 12: 560–567.
42. McQualter JL, Darwiche R, Ewing C, Onuki M, Kay TW, Hamilton JA, *et al*. Granulocyte macrophage colony-stimulating factor: A new putative therapeutic target in multiple sclerosis. J Exp Med 2001, 194: 873–882.
43. Yasuda K, Takeuchi Y, Hirota K. The pathogenicity of Th17 cells in autoimmune diseases. Semin Immunopathol 2019, 41: 283–297.
44. Cha Y, Moon BH, Lee MO, Ahn HJ, Lee HJ, Lee KA, *et al*. Zap70 functions to maintain stemness of mouse embryonic stem cells by negatively regulating Jak1/Stat3/c-Myc signaling. Stem Cells 2010, 28: 1476–1486.
45. Bhargava P, Fitzgerald KC, Calabresi PA, Mowry EM. Metabolic alterations in multiple sclerosis and the impact of vitamin D supplementation. JCI Insight 2017, 2: e95302.
46. Aqel SI, Yang X, Kraus EE, Song J, Farinas MF, Zhao EY, *et al*. A STAT3 inhibitor ameliorates CNS autoimmunity by restoring Teff: Treg balance. JCI Insight 2021, 6: e142376.
47. Yang J, Sundrud MS, Skepner J, Yamagata T. Targeting Th17 cells in autoimmune diseases. Trends Pharmacol Sci 2014, 35: 493–500.
48. Constantinescu CS, Farooqi N, O'Brien K, Gran B. Experimental autoimmune encephalomyelitis (EAE) as a model for multiple sclerosis (MS). Br J Pharmacol 2011, 164: 1079–1106.
49. Wang Z, Zheng Y, Wang F, Zhong J, Zhao T, Xie Q, *et al*. Mfsd2a and Spns2 are essential for sphingosine-1-phosphate transport in the formation and maintenance of the blood-brain barrier. Sci Adv 2020, 6: eaay8627.
50. Moser T, Akgün K, Proschmann U, Sellner J, Ziemssen T. The role of TH17 cells in multiple sclerosis: Therapeutic implications. Autoimmun Rev 2020, 19: 102647.
51. Thakker P, Leach MW, Kuang W, Benoit SE, Leonard JP, Marusic S. IL-23 is critical in the induction but not in the effector phase of experimental autoimmune encephalomyelitis. J Immunol 2007, 178: 2589–2598.
52. Gooderham MJ, Papp KA, Lynde CW. Shifting the focus - the primary role of IL-23 in psoriasis and other inflammatory disorders. J Eur Acad Dermatol Venereol 2018, 32: 1111–1119.

53. Bunte K, Beikler T. Th17 cells and the IL-23/IL-17 axis in the pathogenesis of periodontitis and immune-mediated inflammatory diseases. Int J Mol Sci 2019, 20: 3394.
54. De Simone V, Franzè E, Ronchetti G, Colantoni A, Fantini MC, Di Fusco D, *et al*. Th17-type cytokines, IL-6 and TNF-α synergistically activate STAT3 and NF-kB to promote colorectal cancer cell growth. Oncogene 2015, 34: 3493–3503.
55. Coquet JM, Chakravarti S, Smyth MJ, Godfrey DI. Cutting edge: IL-21 is not essential for Th17 differentiation or experimental autoimmune encephalomyelitis. J Immunol 2008, 180: 7097–7101.
56. Sonderegger I, Kisielow J, Meier R, King C, Kopf M. IL-21 and IL-21R are not required for development of Th17 cells and autoimmunity *in vivo*. Eur J Immunol 2008, 38: 1833–1838.
57. Di Cesare A, Di Meglio P, Nestle FO. The IL-23/Th17 axis in the immunopathogenesis of psoriasis. J Invest Dermatol 2009, 129: 1339–1350.
58. Egeberg A, Gisondi P, Carrascosa JM, Warren RB, Mrowietz U. The role of the interleukin-23/Th17 pathway in cardiometabolic comorbidity associated with psoriasis. J Eur Acad Dermatol Venereol 2020, 34: 1695–1706.
59. Waisman A, Hauptmann J, Regen T. The role of IL-17 in CNS diseases. Acta Neuropathol 2015, 129: 625–637.